ACS Macro Letters

Letter

pubs.acs.org/macroletters

Morphology, Thickness, and Composition Evolution in Supramolecular Block Copolymer Films over a Wide Range of Dip-Coating Rates

Sébastien Roland, Robert E. Prud'homme,* and C. Geraldine Bazuin*

Département de chimie, Centre de recherche sur les matériaux auto-assemblés (CRMAA/CSACS), Université de Montréal, C.P. 6128 succursale Centre-ville, Montréal (QC), Canada H3C 3J7

Supporting Information

ABSTRACT: Dip-coating, an important industrial technique, has been underexploited for preparing block copolymer (BC) thin films, such that the knowledge regarding their general characteristics is limited. Here, we present an overview of the crucial factors that determine how BC film morphology evolves as a function of dip-coating rate (withdrawal speed) over a wide range, illustrated using THF solutions of a polystyrene-*b*-poly(4-vinyl pyridine) (PS-P4VP) diblock copolymer mixed with two small molecules, naphthol and naphthoic acid, which are hydrogen-bonders with P4VP. Key factors in determining the film morphology are the systematic variation in film thickness and, for supramolecular BCs, in film composition with dip-coating rate. The former shows a general V-shaped dependence, related to the so-called capillarity and draining regimes identified previously for dip-coated sol–gel films. The relative small molecule content in the films studied is shown to increase in the capillarity regime from low to that of the dip-coating solution and thereafter to remain constant. Together, these changes, in addition to solvent and other effects, determine the film morphology and its evolution with dip-coating rate.

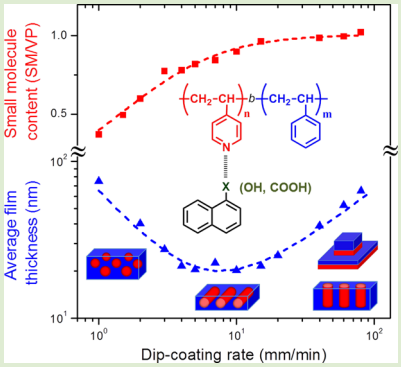

Block copolymer (BC) thin films have been under extensive investigation for many years, due to the fundamental interest in understanding what controls their morphologies and to the various nanotechnological applications that can utilize these morphologies.[1−6] The most common method for preparing BC films for study is by spin-coating, generally followed by annealing. Dip-coating is a frequently used industrial technique for preparing thin films, with advantages such as simplicity of use and little loss of solution,[7] but has received limited attention to date for BCs.[8−17] Here, we present an overview of key factors critical for understanding, controlling and manipulating the general characteristics of BC films dip-coated over a wide range of rates (with no postannealing applied), and show their particular consequences for supramolecular BCs.

Salient findings by the main groups that have investigated dip-coated BCs to date include the following. Krausch and colleagues observed that the morphology of PS-P2VP [polystyrene-*b*-poly(2-vinyl pyridine)] films dip-coated from toluene solution varies with solution concentration,[8,9] and is featureless below a critical dip-coating rate that also depends on solution concentration.[10] Stamm and colleagues showed that the film morphology of supramolecular PS-P4VP (where a functional small molecule, SM, that hydrogen bonds to P4VP is incorporated) depends on the dip-coating solvent used.[11,12] Our group found that the morphology of similar films depends on the SM used for supramolecular control as well as on the dip-coating rate.[16] We will show here that each of these works are limited aspects of a larger, unified picture.

The starting point for an overall understanding is a recent publication by Grosso and colleagues showing how the thickness of inorganic sol–gel films varies over a very wide range of dip-coating rates (withdrawal rates).[7,18] They demonstrated that the film thickness first decreases, reaches a minimum and then increases as a function of dip-coating rate, u. At low rates ("capillarity regime"), the thickness varies as u^{-1} and is governed by capillary feeding and solvent evaporation. At high rates ("draining regime"), which has most often been used for preparing dip-coated films in general,[7] the thickness varies as $u^{2/3}$ and can be described by a draining model developed from the Landau–Levich equation.[19] Together, these regimes give a roughly V-shaped film thickness/dip-coating rate relationship. We will show that this relationship applies equally to BC films and, most importantly, strongly influences their morphology. In addition, the SM content of supramolecular BCs can be strongly influenced by the dip-coating rate, depending on the regime. The morphologies obtained in dip-coated BC films must be understood within this general perspective, using the knowledge gained previously from studies of annealed spin-coated films. Moreover, with this perspective, it is clear that previous investigations of such films by our group have been conducted on the capillarity side of the minimum, whereas those of the Krausch and Stamm groups were conducted on the draining side.

Received: June 21, 2012
Accepted: July 12, 2012
Published: July 16, 2012

The films discussed here are dip-coated from THF solutions containing a PS-P4VP diblock copolymer [M_n(PS) = 41.5 kg/mol; M_n(P4VP) = 17.5 kg/mol] and an equimolar quantity, relative to VP, of 1-naphthol (NOH) or 1-naphthoic acid (NCOOH), which hydrogen bond to P4VP with differing strengths (NCOOH > NOH).[16,17,20] The THF solutions were shown by dynamic and static light scattering to be micellar, with the same spherical micelle shape and size in the presence of either SM or no SM.[16] Dip-coated films were prepared from NOH- and NCOOH-containing solutions with a PS-P4VP concentration of 5 mg/mL, as well as from an NOH solution with twice the concentration (10 mg/mL), and from SM-free PS-P4VP solutions at both concentrations. Withdrawal rates, determined by the limits of the Langmuir film balance used for dip-coating, varied between 1 and 80 mm/min. No postannealing was applied to the films.

Figure 1 shows that the average film thickness varies with dip-coating rate in a V-shaped manner for all five dip-coating

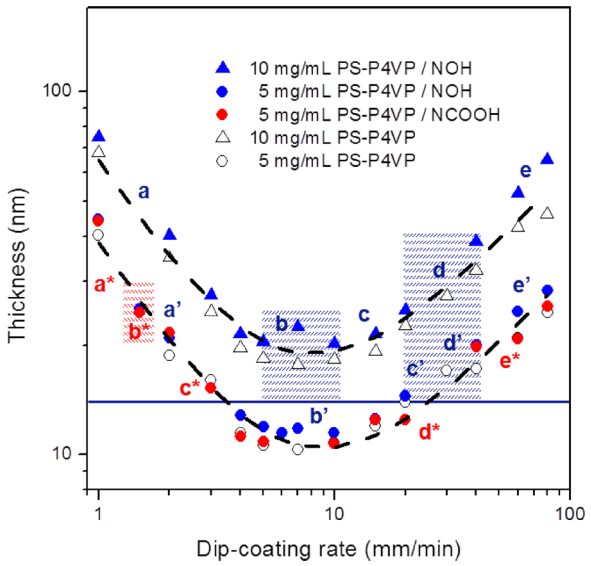

Figure 1. Average film thickness as a function of the rate of dip-coating from THF solutions of the BC concentration and containing the SM indicated (SM/VP = 1.0). The black dashed lines are calculated according to ref 7. The letters refer to the AFM morphology images in Figure 2 and identify the regions along the curves where the indicated morphologies are observed. The hatched areas correspond to the dot/stripe transition regions for films containing NOH (blue) and NCOOH (red). The horizontal blue solid line corresponds to the critical thickness, below which only a brush layer forms.

solutions. The dashed lines through the data points are fits that combine the u^{-1} and $u^{2/3}$ dependencies for the capillarity and draining regimes, respectively (see also Figure S1). They show the general applicability to block copolymer films of the film thickness/dip-coating rate dependence described in ref 7. The type of small molecule, NOH or NCOOH, and even its presence or not, have little or no influence on the film thickness, as shown by the similarity of the three 5 mg/mL solutions and the similarity of the two 10 mg/mL solutions. The difference between the 5 and 10 mg/mL solutions indicates that increasing the solution concentration produces thicker films, as also found for sol–gel films.[7] The minimum thickness for the two concentrations is about 10 and 20 nm, respectively, and occurs over a relatively broad dip-coating rate region around 10 mm/min.

The evolution of the film morphologies along the film thickness curves, summarized by a series of topographical AFM images in Figure 2 (with their location along the curves

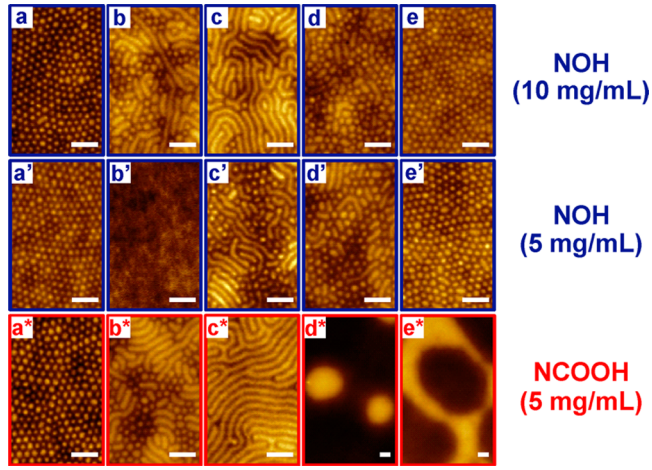

Figure 2. AFM topographic images (scale bars 200 nm) of PS-P4VP/SM films dip-coated from 5 and 10 mg/mL THF solutions. The film thickness/dip-coating rates for each image are indicated in Figure 1 by the corresponding letters, a–e, a′–e′, and a*–e*. For more details, see Figures S2–S4.

indicated in Figure 1) and complemented with larger images of a more complete series in Figures S2–S4, is complex. We will begin with the NOH-containing films. For the 5 mg/mL solution, the film morphology evolves from dots at slow dip-coating rates (capillarity regime), to laterally featureless films at intermediate dip-coating rates (region of minimum thickness), to mixed dots and short stripes, followed by only dots at higher dip-coating rates (draining regime). For the 10 mg/mL solution, the sequence is similar, except that the range giving featureless films for the 5 mg/mL solution now produces mixed dots and stripes on the capillarity side of the film thickness minimum and, on the draining side, almost exclusively long stripes (fingerprint texture), followed by another mixed dot-and-stripe region that evolves to almost exclusively dots. In the capillarity regime, the dot morphology is one of essentially spherical P4VP/SM micelles, determined by the solution characteristics, as indicated by cross-sectional TEM (transmission electron microscopy).[16] In the draining regime, on the other hand, this morphology is more likely one of vertical P4VP/SM cylinders, based on the conclusions of Stamm and colleagues for PS-P4VP films dip-coated in the draining regime from micellar dioxane solutions containing 2-(4′-hydroxyphenylazo) benzoic acid (HABA).[11,12] The stripes must then be horizontal P4VP/SM cylinders,[16] cylinder orientation being related to solvent evaporation rate combined with film thickness effects.[21] The coexisting dot–stripe morphology can be related to being in a morphological transition region.

In the minimum film thickness region, the featurelessness of the PS-P4VP/NOH films dip-coated from the 5 mg/mL solution indicates that only a "brush" layer of copolymer covers the substrate (confirmed by cross-sectional TEM).[16] This brush layer is composed of a P4VP wetting layer adsorbed to the substrate and covered by a PS layer that reduces the interfacial energy with air.[8,16,22] For the 10 mg/mL solution, the higher minimum thickness of the films is greater than that of the brush layer, leading to the appearance of laterally repetitive morphological features over the entire range of dip-coating

dx.doi.org/10.1021/mz3003165 | ACS Macro Lett. 2012, 1, 973–976

rates, particularly the stripe morphology in the thinner films. The critical thickness of PS-P4VP/NOH films, above which the film is composed of more than a brush layer, is represented in Figure 1 by the horizontal solid blue line positioned at about 13 nm. This critical thickness is determined by the block molecular weights combined with interfacial interactions involving the block domains, substrate and air, which are also influenced by the small molecule present.[1,23]

Overall, in the PS-P4VP/NOH films investigated, the morphology evolves from spheres to horizontal cylinders to vertical cylinders of P4VP/SM as a function of withdrawal rate, with a "cutoff" brush-layer morphology present for film thicknesses attaining the brush-layer thickness.

The morphology evolution of NCOOH-containing films as a function of dip-coating rate is quite different from NOH-containing films (5 mg/mL solutions), which is indicative of a contribution of supramolecular control over the morphology. At very slow dip-coating rates, the morphology of both SM-containing films is identical (dots only; i.e., P4VP/SM spheres[16]), but as dip-coating rate increases, the NCOOH-containing films evolve to the stripe morphology (P4VP/SM horizontal cylinders[16]) while still in the capillarity regime. This is followed, in the thinnest films (3−5 mm/min dip-coating), by the coexistence of thin ribbons (about 25 nm in height) characterized mainly by the stripe morphology and lower featureless regions indicative of the brush layer (see Figure S4). At 10 mm/min dip-coating, the predominant brush layer coexists with essentially flat islands (also, about 25 nm in height) that grow and coalesce with dip-coating rate. These "island" and "hole" morphologies are characteristic of flat-on lamellae that form terraces due to incommensurability between film thickness and the natural block periodicity.[1,24] Thus, overall, the morphology in the PS-P4VP/NCOOH films investigated evolves with dip-coating rate from spherical to horizontal cylindrical to flat-on lamellar, again with a "cutoff" brush layer in the thinnest films (although always coexisting with a fraction of additional layer for the rates studied).

An important issue that is particular to supramolecular dip-coated films is how the SM/VP ratio in the films ("uptake ratio") compares to that in solution. This can be determined spectroscopically, particularly by the ATR-IR technique, described in detail elsewhere.[17] Figure 3 shows that the SM/VP uptake ratio varies strongly as a function of withdrawal rate. The variation is identical for NOH- and NCOOH-containing systems and independent of solution concentration within experimental uncertainty. At the slowest rate used, the proportion of SM in the film is very low, at about 20% of the equimolar ratio in solution. It then increases rapidly with dip-coating rate in the capillarity regime to reach about 90% of equimolar in the region of minimum film thickness and full equimolar at about 20 mm/min. Following this, no further change occurs, indicating little or no effect in the draining regime of the dip-coating rate on SM content in the films. In other words, for very slow dip-coating rates in the capillarity regime, the SM has ample time to diffuse out of the meniscus that feeds the depositing film into the bulk solution; that is, it is effectively largely washed out from the depositing film. As the dip-coating rate increases, this effect decreases in importance, to finally disappear in the draining regime where the entrained film has no prolonged contact with the solution, thus, preventing any washing out. The behavior in the capillarity regime can be related to the ability of THF to compete with P4VP as an H-bond acceptor, thus minimizing specific interaction of the SM with P4VP in solution.[25] The behavior may be expected to be quite different in other solvents. Indeed, preliminary results in the capillarity regime using $CHCl_3$, which is not a hydrogen-bond acceptor (but which is a good solvent for both blocks), indicate an essentially constant SM/VP ratio as a function of dip-coating rate (but which is greater for NCOOH than for NOH). The effect of various types of solvents on the SM content in dip-coated films in the capillarity and draining regimes is currently under detailed investigation.

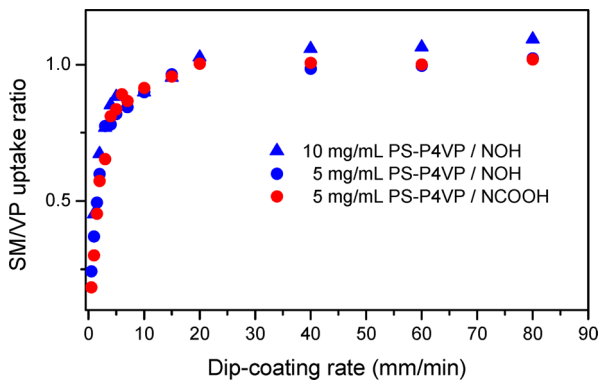

Figure 3. SM/VP uptake ratio, determined by ATR-IR, in PS-P4VP/SM films as a function of the rate of dip-coating from the THF solutions indicated (SM/VP = 1.0).

The evolution of the SM/VP ratio in the films with dip-coating rate is another crucial element, along with film thickness variation, for understanding the evolution in morphology. Because the SM selectively concentrates in the P4VP phase, a change in SM/VP ratio implies a change in volume fraction of the phases, well-known to influence BC morphology.[1−6] Thus, an increase in this ratio, which increases the P4VP/SM volume fraction, explains why the spherical morphology at low rates can transform to a cylindrical (for NOH) and even a lamellar (for NCOOH) morphology at higher dip-coating rates, with morphological orientation determined by the film thickness, solvent evaporation rate, and so on.[21] The contrast in morphology evolution between the NOH- and NCOOH-containing films, despite their having identical SM/VP uptake ratios that evolve identically, is less clearly evident, but must somehow be related to the stronger NCOOH−VP H-bond. One possible consequence is that this can result in greater if not exclusive selectivity of NCOOH for the P4VP phase, whereas a fraction of NOH may be dispersed in the PS phase.[16,17] It is then reasonable that the NCOOH-containing films can attain the conditions for lamellar morphology while the NOH-containing films dip-coated in the same conditions are still characterized by a cylindrical morphology.

In comparison with the films obtained from the SM-containing solutions, films of PS-P4VP dip-coated from SM-free solutions (5 and 10 mg/mL) show only the dot morphology over the entire range of dip-coating rates investigated, with the exception that the thinnest films from the 5 mg/mL solution display coexisting featureless regions indicative again of a brush layer (AFM images given in Figure S5). This apparently constant morphology, which probably reflects spherical micelles, as in the low SM-containing films (although a change from spherical micelles in the capillarity regime to vertically oriented cylinders in the draining regime is not ruled out), can be related to the necessarily constant film

dx.doi.org/10.1021/mz3003165 | ACS Macro Lett. 2012, 1, 973−976

composition. However, other conditions (e.g., other solution concentrations, block ratios, or dip-coating solvent) may lead to a richer morphology evolution in even SM-free films, given that the Krausch group observed featureless, dot, stripe, and mixed morphologies, depending on the solution concentration, in PS-P2VP films (for P2VP block contents ranging from 28−71%) dip-coated in the draining regime from toluene solution.[8,9] A possible explanation in this case is that the morphology is cylindrical in all cases (related to both the BC composition and the solvent used) but that the cylinder orientation varies with film thickness from horizontal in thin films to vertical in thicker films. This would be consistent with what was indicated above for the PS-P4VP/NOH films in the draining regime and with the combined film thickness/solvent evaporation rate dependence of cylinder orientation discussed in ref 21.

To conclude, this communication has shown that the morphology of dip-coated supramolecular diblock copolymer films varies systematically with dip-coating rate, determined particularly by the parallel evolution in film thickness and film composition, along with solution characteristics. The V-shaped thickness evolution is governed by the capillarity and draining regimes described recently for sol−gel films, indicating that this is a general trend for dip-coated films. In supramolecular films, the capillarity process can have a strong effect on the small molecule content in dip-coated films, depending on the nature of the solvent used. In further investigations and for applications of dip-coated BC films, it is crucial to be cognizant of this overall interplay between dip-coating rate, film thickness, and film morphology, as well as film composition in the case of supramolecular BCs, influenced also by the solvent.

■ ASSOCIATED CONTENT

Supporting Information

Experimental details, complementary film thickness versus dip-coating rate graph, additional AFM images. This material is available free of charge via the Internet at http://pubs.acs.org.

■ AUTHOR INFORMATION

Corresponding Author

*E-mail: geraldine.bazuin@umontreal.ca; re.prudhomme@umontreal.ca.

Notes

The authors declare no competing financial interest.

■ ACKNOWLEDGMENTS

This work was supported by NSERC Canada and FQRNT Québec. We thank Prof. Christian Pellerin of our department for access to the infrared instrumentation.

■ REFERENCES

(1) Fasolka, M. J.; Mayes, A. M. *Annu. Rev. Mater. Res.* **2001**, *31*, 323−355.
(2) Hamley, I. W. *Prog. Polym. Sci.* **2009**, *34*, 1161−1210.
(3) Li, M.; Coenjarts, C. A.; Ober, C. K. *Adv. Polym. Sci.* **2005**, *190*, 183−226.
(4) Olson, D. A.; Chen, L.; Hillmyer, M. A. *Chem. Mater.* **2008**, *20*, 869−890.
(5) van Zoelen, W.; ten Brinke, G. *Soft Matter* **2009**, *5*, 1568−1582.
(6) Marencic, A. P.; Register, R. A. *Annu. Rev. Chem. Biomol. Eng.* **2010**, *1*, 277−297.
(7) Faustini, M.; Louis, B.; Albouy, P. A.; Kuemmel, M.; Grosso, D. *J. Phys. Chem. C* **2010**, *114*, 7637−7645. Grosso, D. *J. Mater. Chem.* **2011**, *21*, 17033−17038.
(8) Meiners, J. C.; Ritzi, A.; Rafailovich, M. H.; Sokolov, J.; Mlynek, J.; Krausch, G. *Appl. Phys. A: Mater. Sci. Process.* **1995**, *61*, 519−524.
(9) Li, Z.; Zhao, W.; Liu, Y.; Rafailovich, M. H.; Sokolov, J.; Khougaz, K.; Eisenberg, A.; Lennox, R. B.; Krausch, G. *J. Am. Chem. Soc.* **1996**, *118*, 10892−10893.
(10) Meiners, J. C.; Quintel-Ritzi, A.; Mlynek, J.; Elbs, H.; Krausch, G. *Macromolecules* **1997**, *30*, 4945−4951.
(11) Sidorenko, A.; Tokarev, I.; Minko, S.; Stamm, M. *J. Am. Chem. Soc.* **2003**, *125*, 12211−12216.
(12) Tokarev, I.; Krenek, R.; Burkov, Y.; Schmeisser, D.; Sidorenko, A.; Minko, S.; Stamm, M. *Macromolecules* **2005**, *38*, 507−516.
(13) Nandan, B.; Vyas, M. K.; Böhme, M.; Stamm, M. *Macromolecules* **2010**, *43*, 2463−2473.
(14) Kuila, B. K.; Gowd, E. B.; Stamm, M. *Macromolecules* **2010**, *43*, 7713−7721.
(15) Laforgue, A.; Bazuin, C. G.; Prud'homme, R. E. *Macromolecules* **2006**, *39*, 6473−6482.
(16) Roland, S.; Gaspard, D.; Prud'homme, R. E.; Bazuin, C. G. *Macromolecules* **2012**, *45*, 5463−5476.
(17) Roland, S.; Pellerin, C.; Prud'homme, R. E.; Bazuin, C. G. *Am. Chem. Soc., Polym. Prepr.* **2011**, *52*, 101−102 Full paper submitted to *Macromolecules*..
(18) Le Berre, M.; Chen, Y.; Baigl, D. *Langmuir* **2009**, *25*, 2554−2557.
(19) Landau, L.; Levich, B. *Acta Phys. Chim. U.R.S.S.* **1942**, *17*, 42−54.
(20) Lee, J. Y.; Painter, P. C.; Coleman, M. M. *Macromolecules* **1988**, *21*, 954−960.
(21) Phillip, W. A.; Hillmyer, M. A.; Cussler, E. L. *Macromolecules* **2010**, *43*, 7763−7770.
(22) Karim, A.; Singh, N.; Sikka, M.; Bates, F. S.; Dozier, W. D.; Felcher, G. P. *J. Chem. Phys.* **1994**, *100*, 1620−1629.
(23) van Zoelen, W.; Asumaa, T.; Ruokolainen, J.; Ikkala, O.; ten Brinke, G. *Macromolecules* **2008**, *41*, 3199−3208.
(24) Kim, S.; Nealey, P. F.; Bates, F. S. *ACS Macro Lett.* **2012**, *1*, 11−14.
(25) Huang, W.-H.; Chen, P.-Y.; Tung, S.-H. *Macromolecules* **2012**, *45*, 1562−1569.